Science Advances

Supplementary Materials for

Suppression of osteoclast multinucleation via a posttranscriptional regulation–based spatiotemporally selective delivery system

Qingqing Wang *et al.*

Corresponding author: Shunwu Fan, shunwu_fan@zju.edu.cn; Xin Liu, xinliuzju@zju.edu.cn;
Xianfeng Lin, xianfeng_lin@zju.edu.cn

The PDF file includes:

Tables S1 to S3
Figs. S1 to S11
Legends for data S1 and S2

Other Supplementary Material for this manuscript includes the following:

Data S1 and S2

Supplementary Tables and Figures

Table S1. RT–qPCR primers

Name	Forward (5' to 3')	Reverse (5' to 3')
ciRNA975	GATTTAGATTCCGGGGTGCAC	TTCTGAGATGCCCTGTGGAG
ciRNA963	GCATCATCATGGCAGGAAGT	GCCTTGTGTCTGTACGAAGC
circRNA10657	CCTGTTCAGTCTGAGGCTCA	TGTAGTTGTTGCTGCAGGAG
circRNA10902	CACAAAGACAATGATGGGATTCA	CAGCACCGTGAGCATTGTG
mmu-circ-0001391	GGGGAGACTCTGGCTTTGAA	TTCTTCTATGTATGGCCCAGTG
mmu-circ-0011760	GAAGAGGAAAAGCAACAATCAGA	TGTGTCCTGAGTCTTTGCCA
mmu-circ-0009153	CCTGAAATTCGAGATGGGCA	ACCAGCAGTCTCAGCAGATG
circRNA12046	TTTGCTCGTAGTCCTGCTGA	TTCCCCGTGGCTCCGT
circRNA12368	ACAACAACAACCCTTTCCAA	TCAAACTCATGAAGACTTTC
circRNA12608	CCGCCTGAGGTGCTAC	CACAAGCATGCCTCCATTGT
circRNA12641	TGTTGACATTGGAGCTCGTG	GTGCGAACAAAACTTAGAACCA
circRNA12743	GGGGAAGTAAGGACCAGAGAC	GGCGGTGTCATAATGTCTCTC
circRNA12766	ACAGAGAGGTTGAGCAGGAAA	ATGCCTGTTCCATCTCAGCA
circRNA2770	TGTCGATGCTGAGAATTGTGC	GTTTCCTGTTCTTGCATGGC
circRNA12777	GCAGAAACTTGGCTCTCTCC	CTCAAGTCTTGCAGGGTCCA
circRNA12792	GCACCAGCGTTGCCCCTT	GCTGTCGTAATTCTGCAGGG
mmu-circ-0000295	AGCCATGGATGAAGGACAGT	CCACGCTGGCATAAACTAATTC
mmu-circ-0013887	GGCAAAGTGGATGTCTGGTC	CTCCATCACCAGCTAGCTCA
circRNA150	CCCGCCAGCTACTCAAATTT	CCCAAAACCAGATTCGCCTC
circRNA2225	ACAAAGAAGGAGTGTGGAA	CATATTGCAATAAGGTCTTCC
circRNA4148	TTCATTGACACGGTTGCGAG	TGTCGATGGTACTGCTCTGT
mmu-circ-0004661	ACCAAGACTTTCCTCCCACA	AGACCTTGGGAAGACTGTTTC
mmu-circ-0006932	CAGAAGACAAAGACAGCCCTG	TTGCAGCATACTTGTCCAGC
mmu-circ-0009699	GGAGCAAATGGATGACTGGC	TGAAGCATCCTGTCTTTTCTGT
ciRNA975	GATTTAGATTCCGGGGTGCAC	TTCTGAGATGCCCTGTGGAG
circBBS9	TGGAGTAATGCTAATGAGTTGAGG	GCTGAGACTTCAGGCATGG
has_circBBS9	AGAGGGATTTATGAGTGATTGCT	AGGTCTGACTCTGGGATTGT
TRAF6	GCAGTGAAAGATGACAGCGTGA	TCCCGTAAAGCCATCAAGCA
GAPDH	AGGACACTGAGCAAGAGAGG	GTAGCTGGGCCTCTCTCATT
circ-GAPDH	GTGCTCAACCAGTTAGCTCTC	CCAAATCCGTTGACTCCGAC
Bbs9	CGAGCAAGCCCTTGATATCTG	TCTGCCCATTATCCTTTAGGCA
Ctsk	CCTGTTGGGCTTTCAGCTCT	CCGTTCTGCTGCACGTATTG
Nfatc1	TTCGAGTTCGATCAGAGCGG	AGGTGACACTAGGGGACACA
Acp5	TGGACCCACCGCCAAGATG	CACAGCCACAAATCTCAGGGT
c-fos	CGAAGGGAACGGAATAAGATG	GCTGCCAAAATAAACTCCAG

Cx3cr1	TCGTCTTCACGTTCGGTCTG	CTCAAGGCCAGGTTCAGGAG
Itgax	TTCATCTCCACGTCAAGCCC	TCCACTTTGGGTGGTGAACA
Cd74	GGCTCCACCTAAAGAGCCAC	GGGTGACTTGACCCAGTTCC
S100a10	GGTTTGCAGGCGACAAAGAC	CAGAGGGTCCTTTTGATTTTCCA
Ube2s	ACATGTGCTGCTGACCATCAA	CCCGGGCAGCATACTCTTCA
Jdp2	CCGTCAGGCACATCAGGTTAT	CTGAAGGGTCTGGGATCTGC
mmu-miR-214-3p	TATAacagcaggcacagacaggc	
mmu-miR-423-3p	TATagctcggtctgaggccc	
mmu-miR-96-5p	CGCtttggcactagcattttgct	
mmu-miR-128-3p	CGtcacagtgaaccggtctcttt	
mmu-miR-30d-5p	CGtgtaaacatccccgactggaag	
mmu-miR-30a-5p	CCGtgtaaacatcctcgactggaag	

Table S2. Nucleotide sequences

	Forward (5' to 3')	Reverse (5' to 3')
pGPU6/GFP/Neo-CircBBS9-shRNA	TCATCTCTGGAGGTGGCTGTA	
CircBBS9-siRNA#1	UCUCUGGAGGUGGCUGUACUU	GUACAGCCACCUCCAGAGAUU
CircBBS9-siRNA#2	CAUCUCUGGAGGUGGCUGUTT	ACAGCCACCUCCAGAGAUGTT
CircBBS9-siRNA#3	CUCUGGAGGUGGCUGUACUTT	AGUACAGCCACCUCCAGAGTT
siRNA$^{\text{hsa\_circBBS9}}$	CUACUCUCUGGUGGUUGUATT	UACAACCACCAGAGAGUAGTT
miR-423-3p mimics	AGCUCGGUCUGAGGCCCCUCAGU	UGAGGGGCCUCAGACCGAGCUUU
miR-423-3p inhibitor	ACUGAGGGGCCUCAGACCGAGCU	
miR-423-3p sponge	ACTGAGGGGCCTCAGACCGAGCT	

Table S3 Antibodies used for Western blots

Antibody	Resource
anti-mouse-CTSK	Santa Cruz Biotechnology
anti-mouse-ATPV6D2	Santa Cruz Biotechnology
anti-mouse-NFATc1	Santa Cruz Biotechnology
anti-mouse-MMP9	Santa Cruz Biotechnology
anti-mouse-CD47	Solarbio

anti-mouse-CD9	Proteintech
anti-mouse-DC-STAMP	Novus Biologicals
anti-mouse-Na-K-ATPase	Santa Cruz Biotechnology
anti-mouse-TRAF6	Santa Cruz Biotechnology
anti-mouse-C-Fos	Santa Cruz Biotechnology
anti-mouse-integrin β3	Santa Cruz Biotechnology
anti-mouse-GAPDH	Santa Cruz Biotechnology
anti-mouse-β-actin	Santa Cruz Biotechnology
secondary antibody	Sigma Aldrich
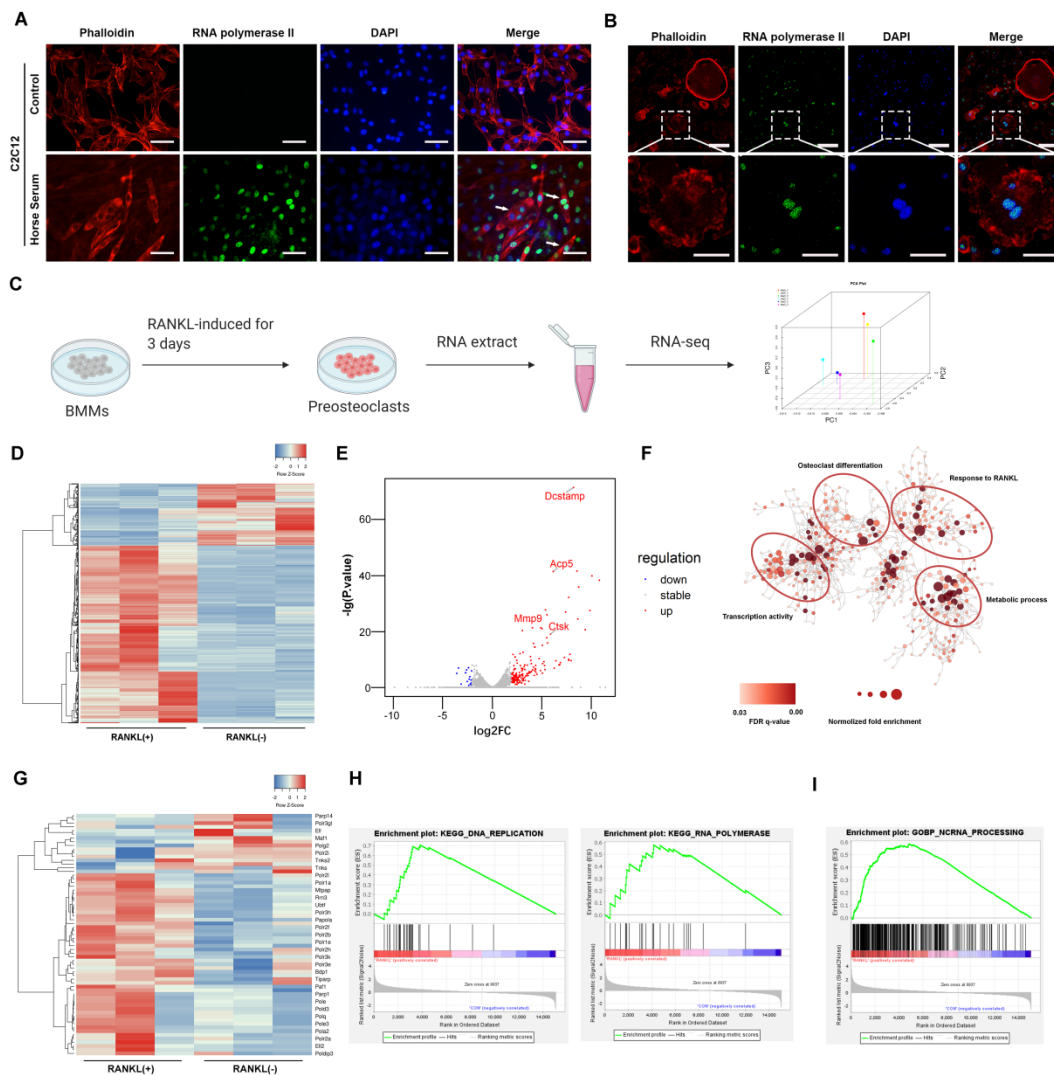
Fig. S1. Transcription patterns in multinucleated cells. (**A**) Representative confocal images of phalloidin and RNA polymerase II subjected to immunofluorescence staining in C2C12 cells with or without horse serum stimulation. Scale bar, 100 μm.phalloidin, red, RNA plymerase II, green; nuclei, blue. (**B**) Representative confocal images of phalloidin and RNA poly II subjected to immunofluorescence staining in pOCs. Scale bar, 100 μm. Enlarged scale bar, 50μm.phalloidin, red, RNA plymerase II, green; nuclei, blue. (**C**) Schematic illustration of RNA-seq of BMMs and preosteoclasts. (**D**) Heatmap analysis of differentially expressed genes between BMMs and pOCs. (**E**) Volcano plot showing the expression profiles between BMMs and pOCs. The red points in the plot indicate marker genes such as Dcstamp, Acp5, Mmp9, and Ctsk. (**F**) The upregulated genes were classified according to their biological processes. (**G**) Heatmap of RNA

polymerase-related gene expression. (**H**) Gene set enrichment analysis (GSEA) was applied to analyze gene sets, including DNA replication and RNA polymerase, between the BMM and pOC groups. (**I**) GSEA demonstrated that the ncRNA process was dramatically upregulated in pOCs.
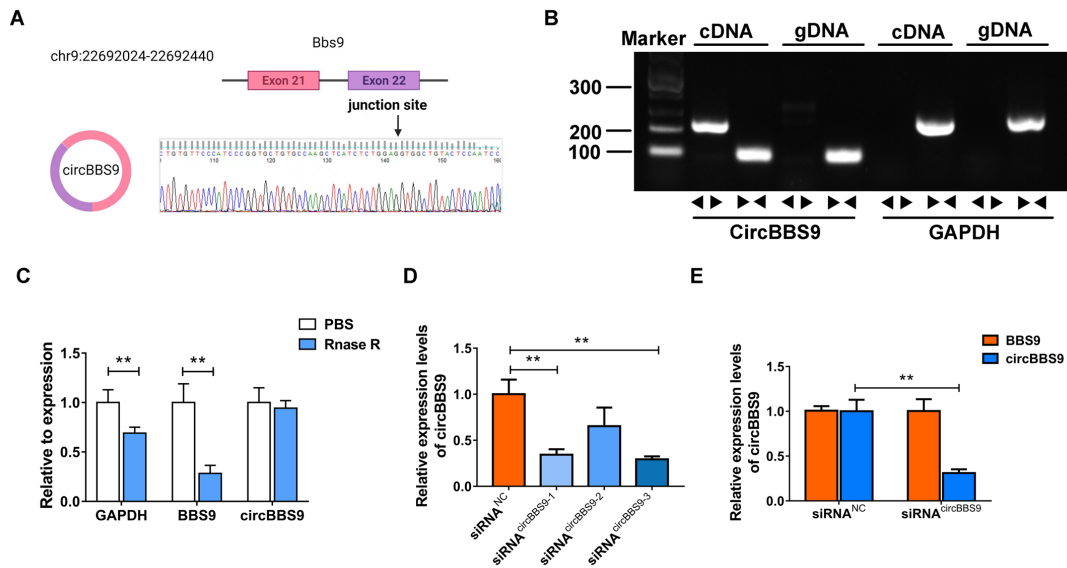
Fig. S2. Identification of circBBS9. (**A**) Sanger sequencing of circBBS9 (**B**) Convergent and divergent primers for circBBS9 or GAPDH were used to verify the closed loop structure by gel electrophoresis. (**C**) Identification of the closed loop structure of circBBS9 via an RNase R tolerance assay. (**D**) Three kinds of siRNAs were verified to knockdown circBBS9 in pOCs. (**E**) Expression of circBBS9 and its linear mRNA after treatment with circBBS9-siRNA in pOCs. $*P < 0.05$, and $**P < 0.01$. The values and error bars are the means ± SDs.
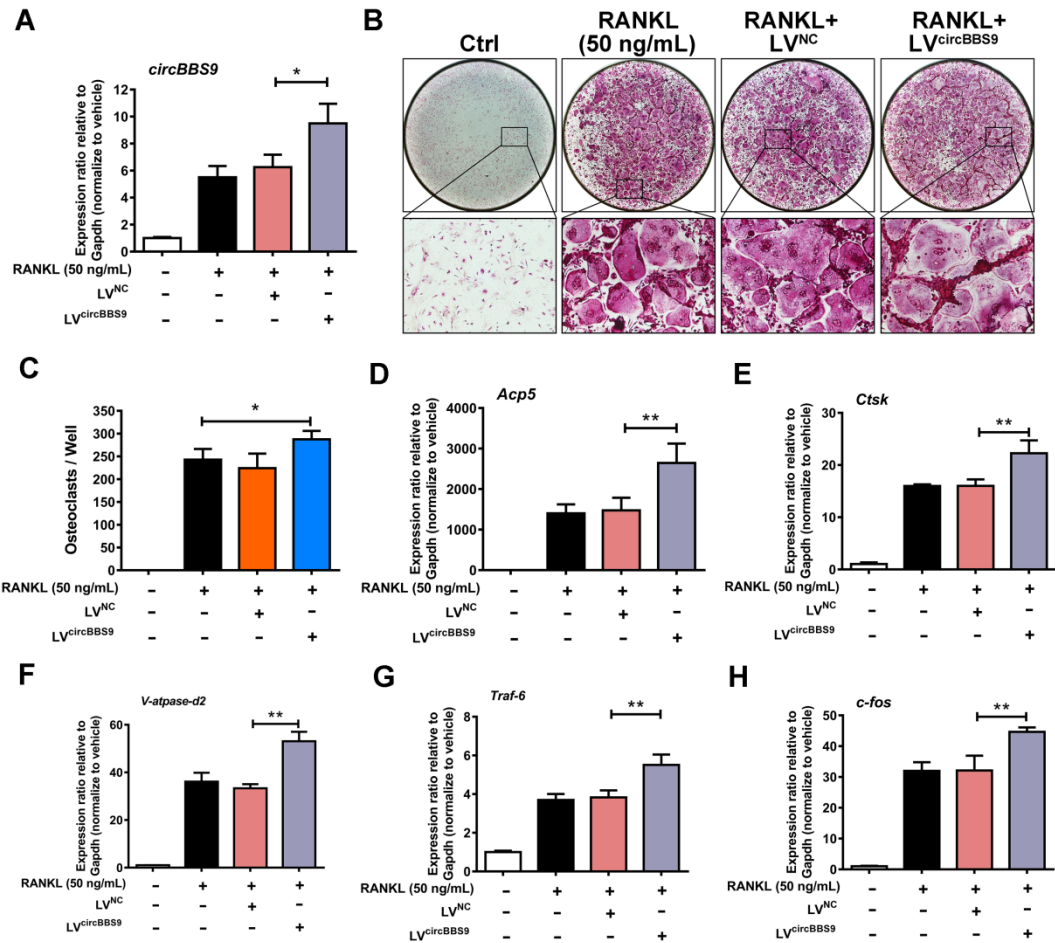
Fig. S3. Effect of overexpression of circBBS9 in osteoclast multinucleation.

(**A**) The expression of circBBS9 after transfection with LV[NC] and LV[circBBS9]. (**B**) Representative images and quantification of TRAP-positive cells per well (in a 96-well plate) in the presence of M-CSF and RANKL for 5 days with transfection with LV[NC] or LV[circBBS9] on day 3. (**C**) The number of TRAP-positive cells (>3 nuclei) was quantitatively analyzed. (**D** to **H**) Gene expression of Acp5, Ctsk, V-atpase-d2, Traf-6, and c-fos in preosteoclasts after transfection with LV[NC] or LV[circBBS9]. Scale bar, 200 μm. *$P < 0.05$, and **$P < 0.01$. The values and error bars are the means ± SDs.
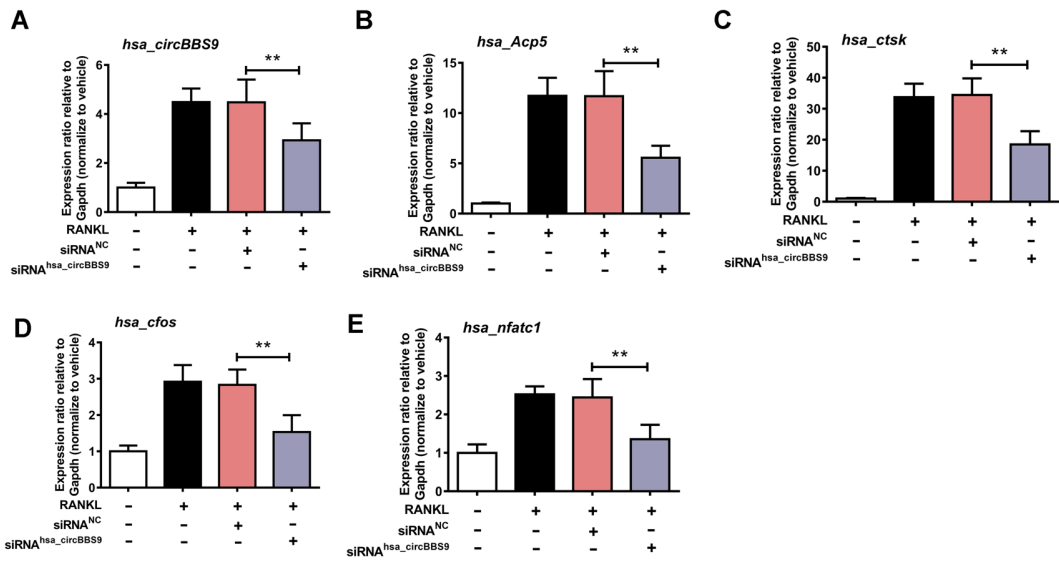
Fig. S4. Effect of knockdown of hsa_circBBS9 in human osteoclast.

(**A**) The expression of hsa_circBBS9 after transfection with siRNA[NC] and siRNA[hsa_circBBs9]. (**B** to **E**) Gene expression of Acp5, Ctsk, c-fos and Nfatc1 in Hum BMM after transfection with siRNA[NC] and siRNA[hsa_circBBs9]. *$P < 0.05$, and **$P < 0.01$. The values and error bars are the means ± SDs.
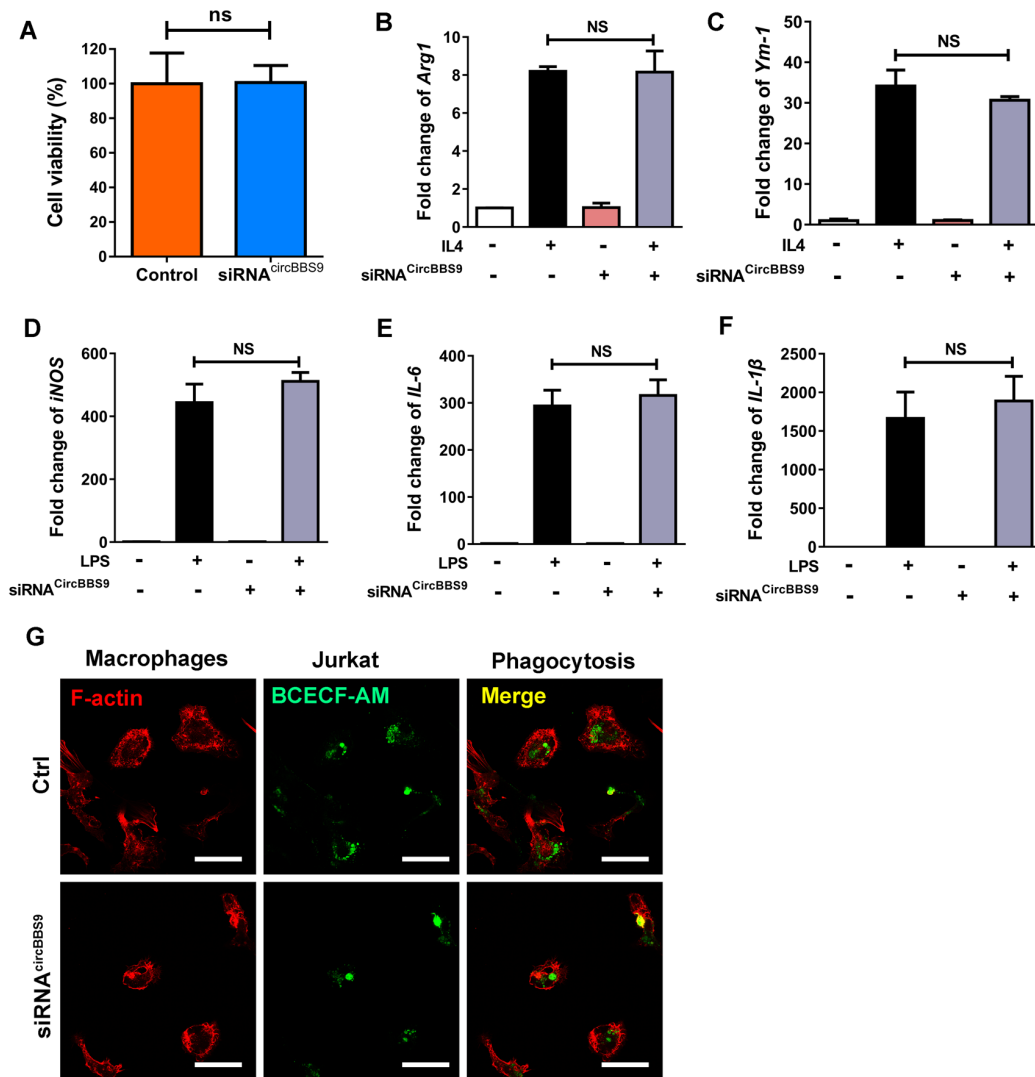
Fig. S5. Effect of siRNA^circBBS9 in macrophage function. (**A**) the cell viability of macrophages measured by CCK-8 with siRNA^circBBS9 treatment. (**B** to **F**) The mRNA expression of Arg1, Ym-1, iNOS, IL-6 and IL-1β with or without LPS and siRNA^circBBS9 treatment (**G**) Macrophages either untreated or treated with siRNAcircBBS9 were incubated with BCECF-AM-labeled apoptotic Jurkat for 2 h. Macrophages, red; Jurkat, green. Scale bar, 50μm.
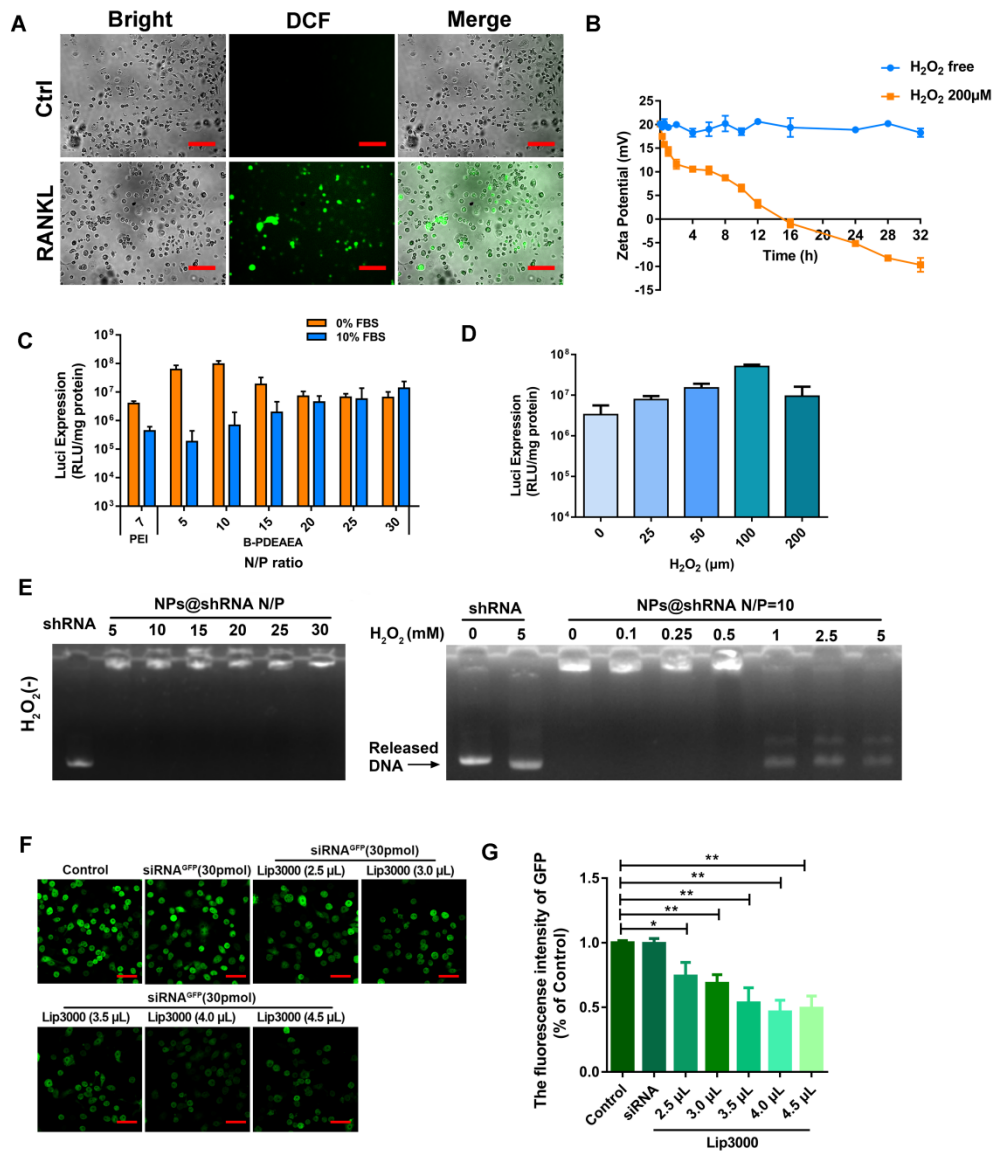
Fig. S6. Preparation of NPs@siRNA/shRNA. (**A**) Intensity of fluorescence showing the levels of ROS in BMMs and pOCs via DCF probe. (**B**) The zeta potential of B-PDEAEA with or without H_2O_2. (**C**) Luciferase expression in RAW264.7 cells of NPs at different N/P ratios with or without 10% serum-containing medium. (**D**) Luciferase expression of NPs in RAW264.7 cells at a 10 *N/P* ratio after 0, 25, 50, 100, and 200 μM H_2O_2 treatment. (**E**) Gel retardation assay of NPs@shRNA at designed N/P ratios after 1 h of incubation with or without H_2O_2 at 37 °C. (**F** and **G**) Representative images and quantification of GFP intensity by siRNA transfection with different concentration of Lipo3000. *$P < 0.05$, and **$P < 0.01$. The values and error bars are the means ± SDs.
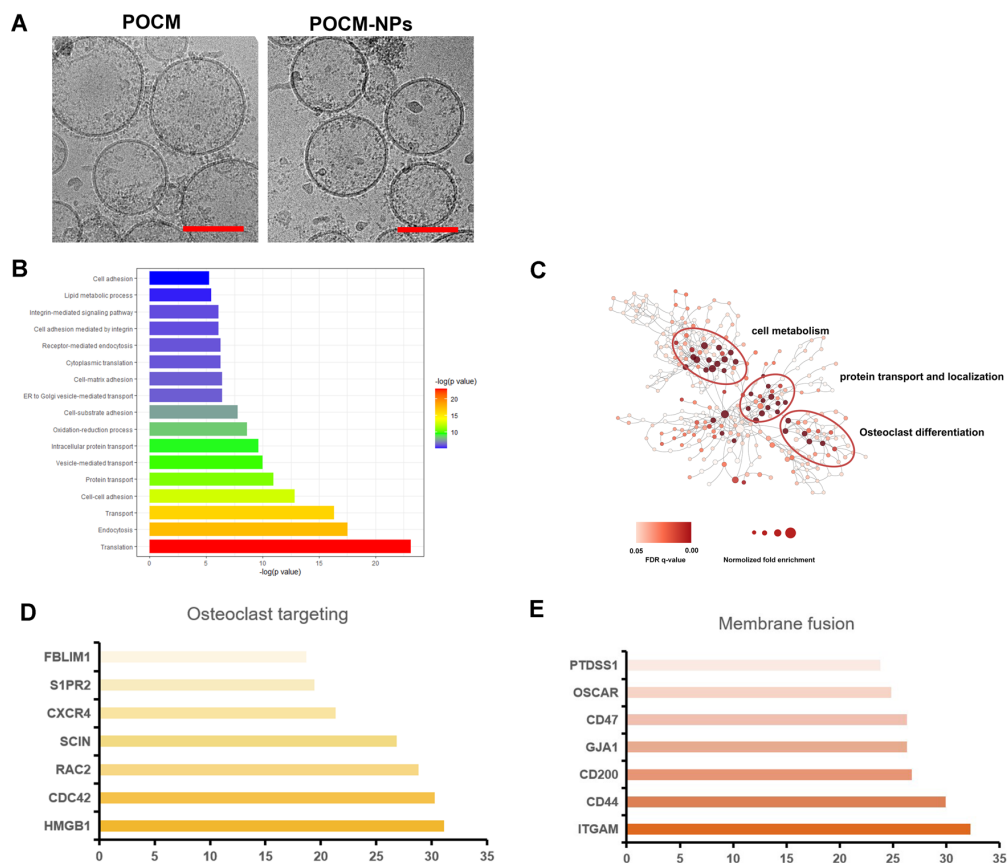
Fig. S7. Image and proteomic analysis of POCM. (**A**) General images of POCM and POCM-NPs by cryo-EM. Scale bar 100nm. (**B**) Bar plot of Gene Ontology biological processes (BP). (**C**) Upregulated genes were classified according to biological processes. (**D** and **E**) Expression of osteoclast targeting- and fusion-related proteins in the pOC membrane.
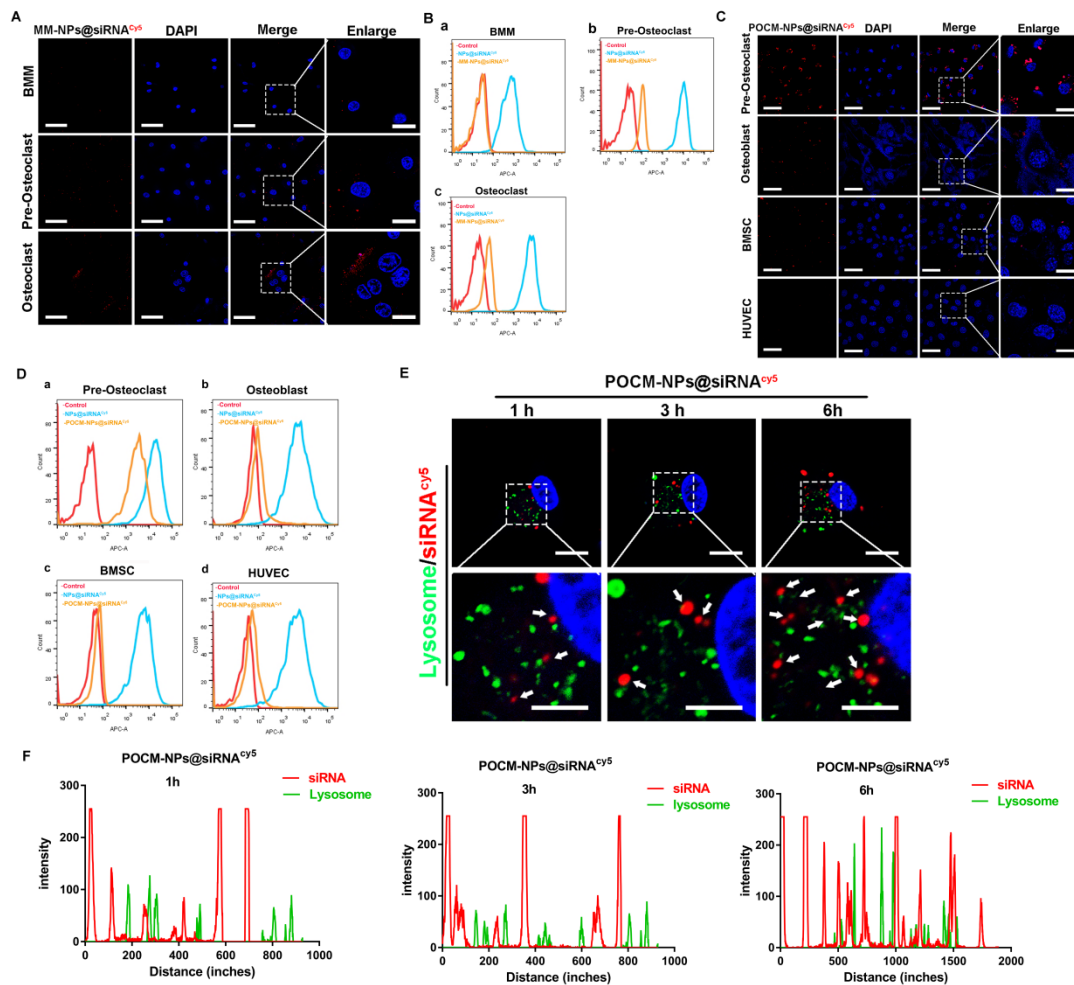
Fig. S8. Self-recognized binding and fusion-mediated intracellular release of POCM-NPs@siRNA.

Representative fluorescence visualization showing low binding efficiency of Cy5-labeled MM-NPs@siRNA[cy5] in BMMs, pOCs, and mOCs. Scale bar, 50 μm. Enlarged scale bar, 20 μm. RNA, red. (**B**) Cy5-positive BMM, pre-osteoclast and osteoclast measured by flow cytometry after treatment of MM-NPs@siRNAcy5. (**C**) Representative fluorescence images of Cy5-labeled POCM-NPs@siRNA[cy5] uptake by preosteoclast, osteoblast, BMSC, and HUVECs. Scale bar, 50 μm. Enlarged scale bar, 20 μm. RNA, red; nuclei, blue. (D) Cy5-positive preosteoclast, osteoblast, BMSC and HUVEC were measured by flow cytometry after treatment of POCM-NPs@siRNA[cy5]. (**E and F**) Fluorescent visualization of siRNA[cy5] and lysosome localization in pOCs after incubation with POCM-NPs@siRNA[cy5] for 1 h, 3 h, and 6 h. And intensity profiles

across the cell along the selected line (indicated by a yellow line in the inset image). Scale bar, 10 μm. Enlarged scale bar, 5 μm. RNA, red; nuclei, blue; lysosome, green.
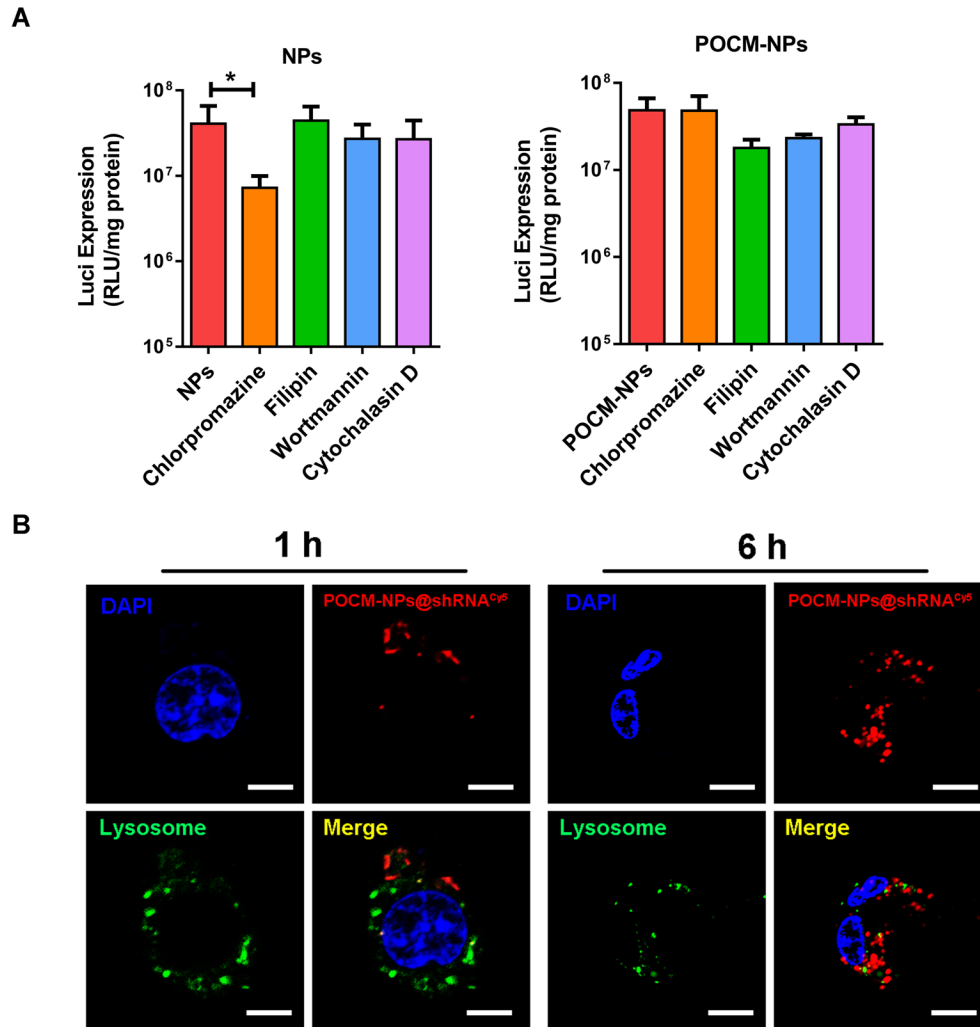
Fig. S9. Intracellular release of POCM-NPs@siRNA/shRNA.

(**A**) The luciferase gene transfection efficiency of NPs or POCM-NPs in pOCs after 48 h. pOCs were separately pretreated with endocytosis-related inhibitors for 0.5 h at 37 °C. (**B**) Fluorescence visualization of shRNA[cy5] and lysosome localization in pOCs after incubation with POCM-NPs@shRNA[cy5] for 1 h and 6 h. Scale bar, 10 μm. RNA, red; nuclei, blue; lysosome, green.
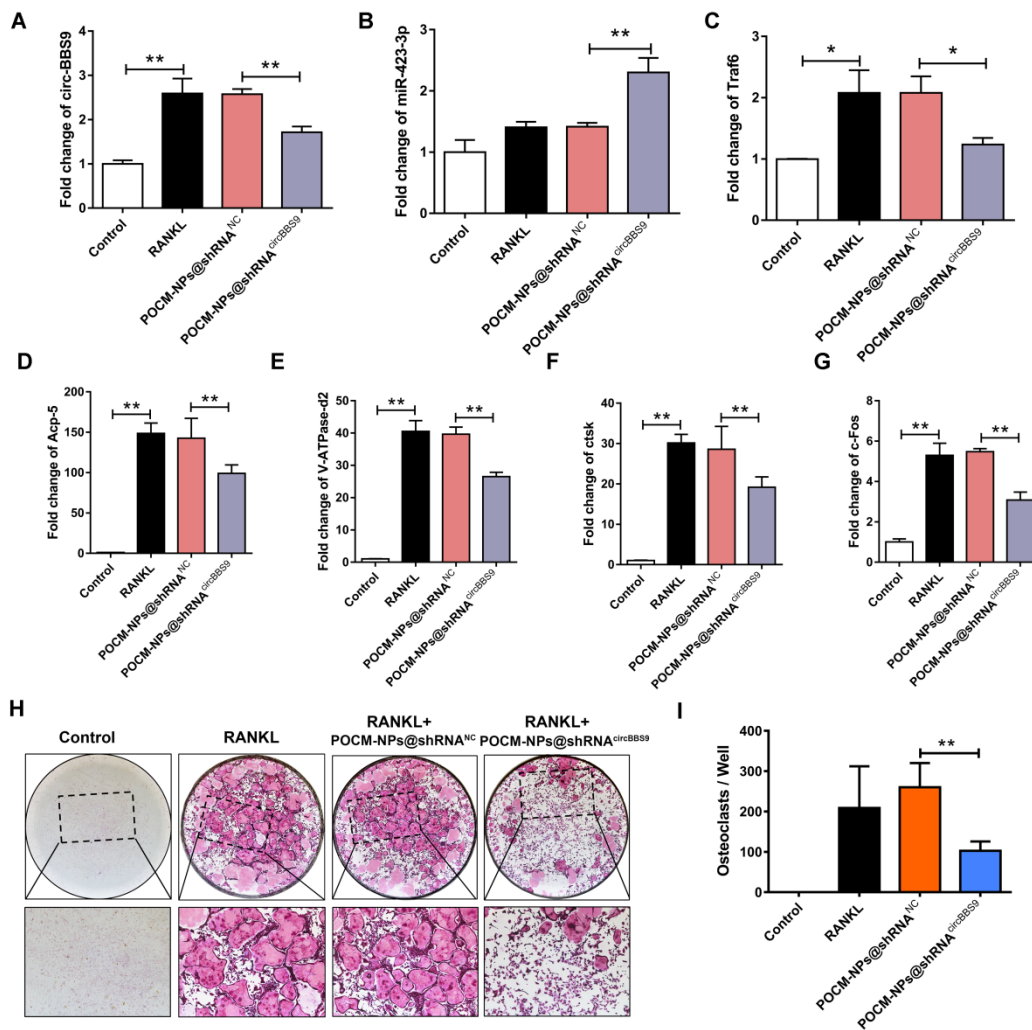
Fig. S10. Gene silencing of POCM-NPs@shRNA^{circBBS9}. (**A** to **C**) Expression of circBBS9, miR-423-3p, and Traf6 detected by RT-qPCR. (**D** to **G**) **Expression of Acp5, V-atpase-d2, Ctsk and c-fos the presence of M-CSF and RANKL for 5 days after transfection with POCM-NPs@shRNA^{circBBS9} or shRNA^{NC}.** (**H**) Representative images and quantification of TRAP-positive cells per well (in a 96-well plate) in the presence of M-CSF and RANKL for 5 days with transfection with shRNA^{circBBS9} or shRNA^{NC} on day 3. (**I**) The number of TRAP-positive cells (>3 nuclei) was quantitatively analyzed. Scale bar, 200 μm. *$P < 0.05$, and **$P < 0.01$. The values and error bars are the means ± SDs.
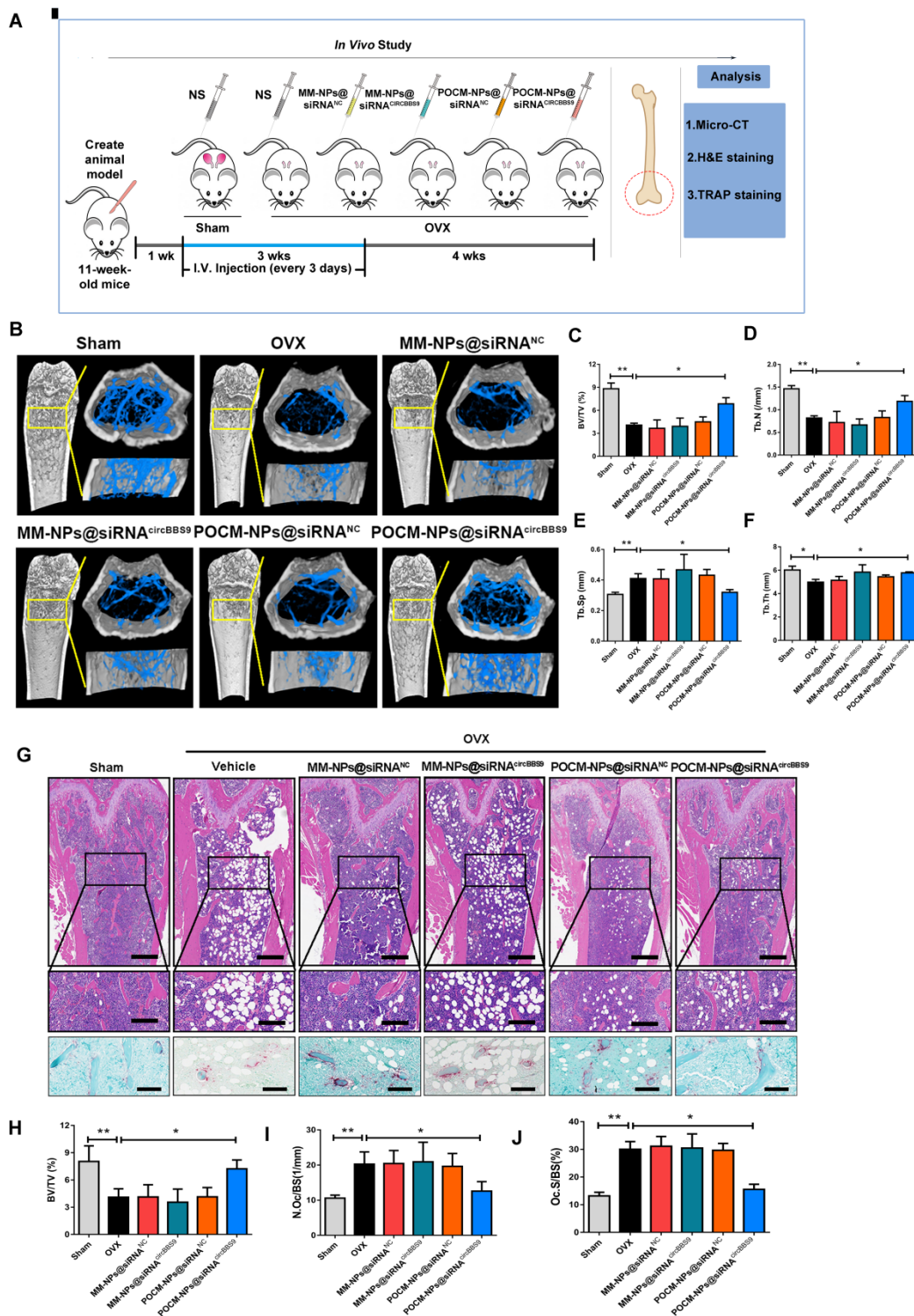
Fig. S11. Preventive effect on osteoporosis of POCM-NPs@siRNA^circBBS9. (**A**) Schematic illustration of the process and group division of animal experiments. (**B**) Micro-CT evaluation of the femur and tibia bone mass in each group. (**C** to **F**) Quantitative measurements of bone microstructure-related parameters, such as BV/TV, Tb.Sp, Tb.N, and Tb.Th, in the sham, PBS, MM-NPs@siRNA^NC, MM-

NPs@siRNA^{circBBS9}. POCM-NPs@siRNA^{NC} and POCM-NPs@siRNA^{circBBS9} groups. (**G** to **J**) H&E and TRAP staining images and quantitative statistics of BV/TV, osteoclast number per bone surface (OC.N/BS), and osteoclast surface area per bone surface (OC.S/BS) in each group. Scale bar, 400 μm. Enlarged scale bar, 200 μm. *$P < 0.05$, and **$P < 0.01$. The values and error bars are the means ± SDs.

Other Supplementary Material for this manuscript includes the following:

Data file S1.

mRNA profile of BMMs and pOCs by RNA-seq.

Provided as a separate Excel file.

Data file S2.

Proteomics profile of BMMs and pOCs by mass spectrometry.

Provided as a separate Excel file.